JOURNAL OF STRUCTURAL BIOLOGY **118,** 23–30 (1997)
ARTICLE NO. SB963837

The Crystal Structure of the Complex of Concanavalin A with 4′-Methylumbelliferyl-α-D-glucopyranoside

STAVROS J. HAMODRAKAS

Department of Biology, Section of Cell Biology and Biophysics, University of Athens, Panepistimiopolis, Athens 157 01, Greece

PANAGIOTIS N. KANELLOPOULOS

Structural Biology Programme, European Molecular Biology Laboratory, D-69012 Heidelberg, Germany

KYRIAKI PAVLOU

Department of Biology, Section of Cell Biology and Biophysics, University of Athens, Panepistimiopolis, Athens 157 01, Greece

AND

PAUL A. TUCKER

Structural Biology Programme, European Molecular Biology Laboratory, D-69012 Heidelberg, Germany

Received August 26, 1996, and in revised form November 22, 1996

Concanavalin A (Con A) is the best known plant lectin, with important biological properties arising from its specific saccharide-binding ability. Its exact biological role still remains unknown. The complex of Con A with 4′-methylumbelliferyl-α-D-glucopyranoside (α-MUG) has been crystallized in space group $P2_1$ with cell dimensions $a = 81.62$ Å, $b = 128.71$ Å, $c = 82.23$ Å, and $\beta = 118.47°$. X-ray diffraction intensities to 2.78 Å have been collected. The structure of the complex was solved by molecular replacement and refined by simulated annealing methods to a crystallographic *R*-factor value of 0.182 and a free-*R*-factor value of 0.216. The asymmetric unit contains four subunits arranged as a tetramer, with approximate 222 symmetry. A saccharide molecule is bound in the sugar-binding site at the surface of each subunit, with the nonsugar (aglycon) part adopting a different orientation in each subunit. The aglycon orientation, although probably determined by packing of tetramers in the crystal lattice, helps to characterize the orientation of the saccharide in the sugar-binding pocket. The structure is the best determined α-D-glucoside:Con A complex to date and the hydrogen bonding network in the saccharide-binding site can be described with some confidence and compared with that of the α-D-mannosides.

INTRODUCTION

Concanavalin A (Con A) is a representative member of the lectin class of plant proteins. It generally exhibits specificity for saccharides containing α-D-mannose or α-D-glucose residues but it may also bind oligosaccharide sequences lacking these units (Goldstein and Poretz, 1986). Con A has specific biological activities which depend on its binding to cell surface receptors. It agglutinates cells transformed by oncogenic viruses, inhibits growth of malignant cells in animals, and exhibits mitogenic activity. Although the exact biological role of Con A remains unknown, its specific saccharide-binding properties make it an ideal object for the study of protein–saccharide interactions.

In solution Con A forms monomers, dimers, or tetramers depending on pH and temperature conditions (Agrawal and Goldstein, 1986) but, at physiological pH, it exists as a tetramer. Each subunit consists of 237 residues and contains two metal sites necessary for saccharide binding (Goldstein and Poretz, 1986). One site binds transition metal ions, notably manganese, while the other binds calcium preferentially.

High-resolution structures of Con A with different metal ions have been determined (Hardman *et al.*, 1982; Weisgerber and Helliwell, 1993; Naismith *et al.*, 1993; Emmerich *et al.*, 1994) and the high-

1047-8477/97 $25.00

resolution structure determination of the Con A methyl-α-D-mannopyranoside complex (α-MM; Naismith *et al.*, 1994) has allowed a detailed description of the mannoside binding site. An essentially identical saccharide binding site is observed for the 4′-nitrophenyl-α-D-mannopyranoside complex (Kanellopoulos *et al.*, 1996). More recently the complex of Con A with the trimannoside core found in N-linked glycans has been described (Naismith and Field, 1996) and provides the reasons for the high affinity of Con A for these glycans.

Our studies are focused on the modes of binding of Con A to a series of saccharides which consist of a mannoside or a glucoside group (saccharide residue) bonded to a second hydrophobic group (aglycon residue). We are trying to examine the role of the nature of the aglycon group in binding. Different binding constants, determined experimentally (Farina and Wilkins, 1980, and references therein; Troganis, 1992), may reflect the assistance brought in binding by the aglycon. Suitable crystals of Con A–saccharide complexes of good quality have been produced for a series of such compounds, which diffract at medium resolution, and X-ray diffraction data have been collected for several complexes. Previously we (Kanellopoulos *et al.*, 1996) have reported the crystal structures of complexes of Con A with 4′-nitrophenyl-α-D-mannopyranoside (α-PNM) and 4′-nitrophenyl-α-D-glucopyranoside (α-PNG) and report here the structure of the complex with 4′-methylumbelliferyl-α-D-glucopyranoside (α-MUG) at 2.78 Å resolution. This allows us to describe with somewhat more confidence the way in which Con A binds to glucosides and to suggest why Con A has a higher affinity for mannosides than for glucosides.

MATERIALS AND METHODS

Purification and Crystallization

The protein was prepared as previously described (Kanellopoulos *et al.*, 1996) and a Con A solution at a concentration of 70 mg/ml was used for cocrystallization experiments with the saccharide α-MUG obtained commercially from Sigma and used without further purification. A ten times molar excess of the saccharide was used to ensure high occupancy in crystals of the complex. The crystals were grown using the hanging drop vapor diffusion method. The reservoir solution contained a 10 m*M* Tris, pH 8.5, 1 *M* $(NH_4)_2SO_4$ solution. The drop was composed of a 1:1 mixture of the well solution with the Con A/saccharide solution. The final volume of the drop was approximately 10 μl. The crystals are monoclinic prisms, with maximum dimensions $0.5 \times 0.4 \times 0.3$ mm and grow after 2 to 3 weeks. They are monoclinic and belong to space group $P2_1$. The unit cell dimensions for the α-MUG complex crystals are $a = 81.62$ Å, $b = 128.71$ Å, $c = 82.23$ Å, and $\beta = 118.47°$. The asymmetric unit contains one Con A tetramer.

Data Collection and Structure Solution

X-ray diffraction data from a single crystal of the Con A–α-MUG complex were collected at room temperature to 2.78 Å on a 18-cm MAR Research image plate detector. Pyrolytic graphite-monochromatized CuK_α radiation ($\lambda = 1.5418$ Å) was used, produced by a rotating anode generator running at 40 kV, 90 mA. The crystals were kept at room temperature (ca. 295K) during data collection. The rotation method was employed and 1° oscillation data frames were collected. The X-ray data were processed using the program XDS (Kabsch, 1988). A summary of the data collection statistics is given in Table I.

The 2.78-Å Con A–α-MUG structure was solved by molecular replacement, using the 2.75-Å model of the concanavalin A/4′-nitrophenyl-α-D-mannopyranoside complex (Kanellopoulos *et al.*, 1996). The 4′-nitrophenyl-α-D-mannopyranoside and all water molecules were omitted from the initial search model. All rotational and translational searches were carried out with the program AMoRe (Navaza, 1994). The fast rotation function calculation was used to determine the orientation of the Con A tetramer in the asymmetric unit. Using reflections in the resolution range 50 to 2.78 Å, and an integration radius of 45 Å, a set of four dominant peaks appeared. The highest of the four peaks was 23 σ and the remaining three had slightly lower values, while the next peak in the list was only 3.5 σ. The set of the four peaks is related by the approximate 222 symmetry of the Con A tetramer; therefore, only one peak was chosen. The translation function calculations were also performed, again with the tetramer as search model, using reflections from 50 to 2.78 Å. A single peak in the translation function, corresponding to a crystallographic *R*-factor of 0.399, was identified for the rotation function solution. The rigid body refinement procedure, implemented in AMoRe, was applied. An initial crystallographic *R* factor of 0.349 was calculated in the resolution range 15–2.78 Å, for a tetramer per asymmetric unit.

Refinement and Model Building

The model was further refined using the program X-PLOR (Brunger, 1992a). During the initial stages of refinement and model building, the four noncrystallographically related molecules in the asymmetric unit were treated independently. Initially the model was subjected to rigid body refinement. Each of the subunits was treated as a separate rigid group and the refinement was performed for all data between 8.0 and 2.78 Å. After this stage, $2F_o$-F_c and F_o-F_c electron density maps were calculated and electron density for the saccharide was clearly identified for all four subunits of the tetramer. Electron density for the saccharide was present in both maps even at a contouring level of five times the rms electron density. The model for α-MUG was built into the density, using the program O (Jones *et al.*, 1991), the accurate geometry of α-PNM (Agianian *et al.*, 1996), and simple geometric calculations. The model was then subjected to further refinement with X-PLOR. The topology and parameter files were adjusted to accommodate the non-proline cis peptide (Ala207-Asp208) and the α-MUG in each subunit. No restraints were placed on metal–ligand distances and no charge was attributed to the metal ions. A step of refinement included simulated annealing refinement with a starting temperature of 3000 K, 120 cycles of conjugate gradient minimization, 15 cycles of overall *B*-factor refinement, 20 cycles of restrained individual *B*-factor

TABLE I
Summary of Data Collection

Resolution range (Å)	48.0–2.78 Å	2.9– 2.78
Observed reflections	151116	
Unique reflections	37358	
Completeness (%)	99.0	95.2
% of observation with $I > 3\sigma(I)$	85.2	62.8
R_{sym} (%)[a]	7.4	23.8

[a] $R_{sym} = \Sigma_{\mathbf{h}}\Sigma_i |F_i^2(\mathbf{h}) - \langle F^2(\mathbf{h})\rangle| / \Sigma_{\mathbf{h}}\Sigma_i F_i^2(\mathbf{h})$.

refinement, and, finally, a further 160 cycles of conjugate gradient minimisation (positional refinement). No I/σ(I) cutoff was applied and 90% of the data in the resolution range 8.0 to 2.78 Å were used in refinement. In order to cross-validate in reciprocal space, the free-*R* value (Brunger, 1992b) was monitored during all steps of refinement using the remaining 10% of the data. However, all data were used for the calculation of $2F_o$-F_c and F_o-F_c electron density maps. Model improvement was then performed for the polypeptide chain and saccharide molecules and refined as described above. Water molecules in the coordination sphere of Mn and Ca ions were added to the model as well as water molecules in the neighborhood of the saccharides. A total of 162 water molecules were included corresponding to peaks in the F_o-F_c electron density map higher than 3.0 times the rms electron density. There were 160 cycles of positional refinement performed on the resulting model. At this resolution, no further attempt to find water molecules was regarded as justifiable. Superposition of subunits showed essentially identical conformations of main chain and side chains for the majority of the protein. Final refinement cycles were performed applying NCS restraints for the metal ions and the Con A subunits, excluding the loops Tyr12–Pro23, Leu115–Asn124, Thr147–Asn153, Ile181–Ser190, Phe199–Ala207, and Pro222–Gly231. Neither the α-MUG nor the water molecules were restrained by the NCS operators. As expected, the conventional *R* factor increases somewhat, indicating some degree of overfitting in the unrestrained refinement. The drop in free-R factor is probably due to loss of independence of cross-validation when NCS restraints are used (Kleywegt, 1996) rather than to a genuine improvement of the model. The refinement statistics are shown in Table II.

RESULTS AND DISCUSSION

Accuracy and Quality of the Model

For clarity, the connectivity of α-MUG together with the used numbering scheme is shown in Fig. 1. The basic topology of the Con A tetramer is unchanged from previously reported Con A structures (e.g., Kanellopoulos *et al.*, 1996) and will not be discussed here. Each tetramer contains two dimers: one dimer is formed by subunits A and B and the other by subunits C and D. The secondary structure elements and folding architecture of each subunit have been discussed in detail and in Con A–α-MUG there are no significant deviations from the reported structures of Con A (e.g., Naismith *et al.*, 1993, 1994;

TABLE II

Summary of Refinement of Con A–α-MUG Complex

Stage	Resolution Range (Å)	*R* factor	*R* free
Molecular replacement solution (AMoRe)	15.0−2.78	0.399	—
Rigid body refinement (XPLOR)	6.0−2.78	0.292	0.298
Addition of four saccharide molecules and SA refinement (XPLOR)	8.0−2.78	0.198	0.255
Addition of 162 water molecules and positional refinement (XPLOR)	8.0−2.78	0.172	0.229
NCS restraints applied (see text)	8.0−2.78	0.182	0.216

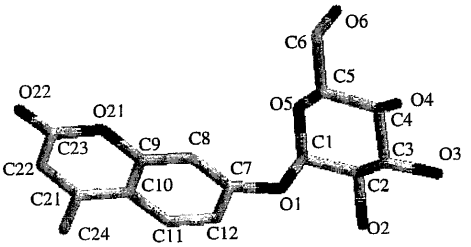

FIG. 1. Chemical formula and atom numbering of 4′-methylumbelliferyl-α-D-glucopyranoside (α-MUG).

Kanellopoulos *et al.*, 1996) and other legume lectins (Reeke and Becker, 1988; Delbaere *et al.*, 1993; Bourne *et al.*, 1992; Shaanan *et al.*, 1991; Rini *et al.*, 1993; Loris *et al.*, 1994; Bourne *et al.*, 1994). Dimer and tetramer formation and stabilization have also been analyzed in detail (Naismith *et al.*, 1993, 1994) and will not be discussed further. Suffice it to say that the tetramer exhibits approximate 222 symmetry. The coordinates have been deposited with the Brookhaven Protein Data Bank as entry 1CJP.

The final 2.78-Å F_o-F_c electron density map calculated omitting the saccharide and water molecules is shown in Fig. 2. This shows the region of the saccharide-binding sites of the C subunit and of the other subunits of symmetry-related tetramers. The aglycon portion of α-MUG appears to be well ordered in all four subunits, with the poorest density for the aglycon part of the sugar in subunit A (Fig. 2). This probably arises because the aglycon of subunit A has more librational freedom than the other subunits, where the aromatic rings are packed parallel to each other (see below).

The structure has good stereochemistry with rms deviations from ideality of 0.008 Å for bond lengths and 1.9° for bond angles. The maximum expected error in atomic positions is estimated to be between 0.25 and 0.30 Å, at 2.78 Å resolution, based on a Luzatti plot (Luzatti, 1952). No residues lie in the disallowed regions, and five residues in the generously allowed regions, of the Ramachandran plot as calculated with the program PROCHECK (Laskowski *et al.*, 1993). The pattern of temperature factors (data not shown) is consistent for main chain and side chain atoms in the same subunit. As expected given the use of NCS restraints, the temperature factors are consistent between subunits and with the real space fit patterns calculated with the program O (data not shown).

Saccharide Binding

As we have previously noted, the saccharide-binding site of Con A exhibits a negative electrostatic potential as calculated with GRASP (Nicholls *et al.*, 1991, 1993, shown for subunit A in Fig. 3b). Upon

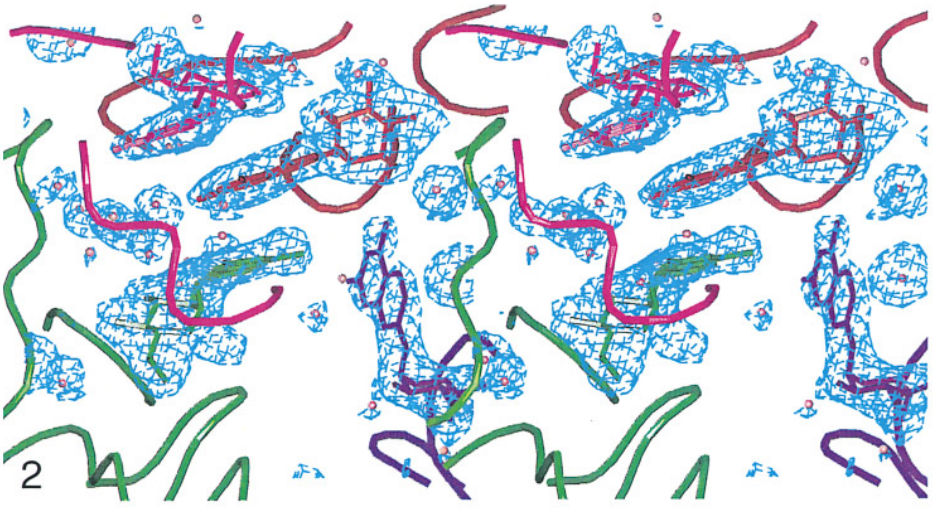
2

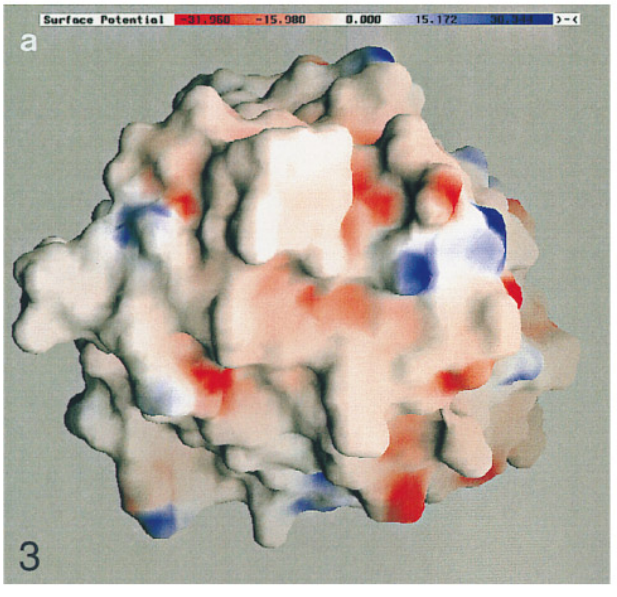
Surface Potential
a
3

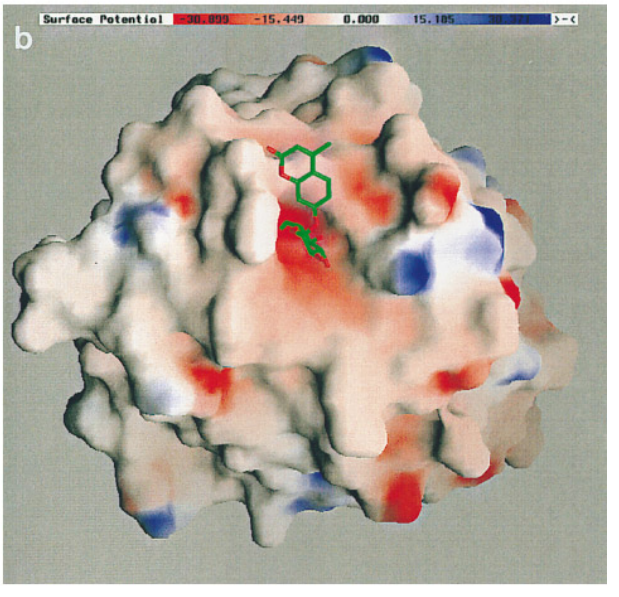
Surface Potential
b

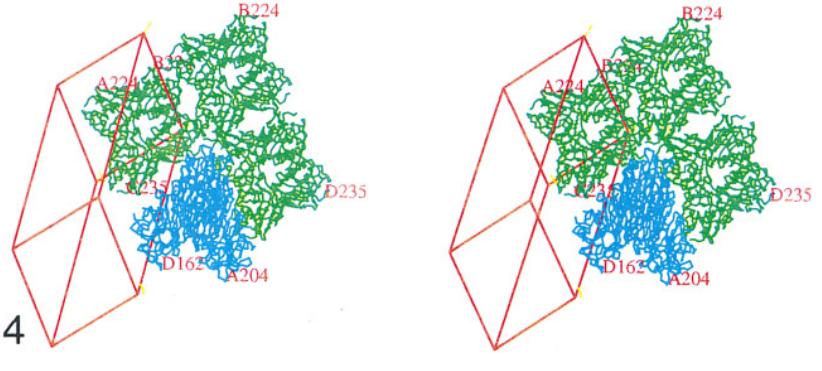
B224
A224
D235
D162
A204
4

binding of the saccharide this negative electrostatic surface is covered (Fig. 3a) by the charge neutral saccharide. These figures also show that although the aglycon group follows the trisaccharide-binding groove (Naismith and Field, 1996) approximately, it neither fills it nor does it cover the more electrostatically negative part of the surface of this groove. 4′-Methylumbelliferyl-α-D-glucopyranoside has conformational flexibility due to possible rotation around two bonds between the saccharide and aglycon group, whereas in the trisaccharide complex there is additional flexibility due to possible rotation around three bonds between the 1,6-terminal mannose and the reducing sugar.

The sugar part of the molecules has a $^4C_1$ chair conformation and the aglycon parts are packed against the hydrophobic portions of the surface of the protein. It has been estimated (utilizing the program WHATIF; Vriend, 1990) that between 158 and 178 Å^2 of water-accessible surface area of the protein is "buried" when it interacts with α-MUG for each subunit of the tetramer. The largest area (178 Å^2) is "buried" for subunit C. Although the differences are probably determined primarily by packing considerations, these values are similar to but slightly larger than those calculated for α-PNM and α-PNG (151 and 149 Å^2, respectively; Kanellopoulos *et al.*, 1996a). Major contributors to these accessibility losses are, in descending order, the side chains of Leu99, Tyr12, Tyr100, and Arg228, although the relative order varies slightly from subunit to subunit. In this context we note that the association constant of α-MUG to Con A is similar to that of α-PNM (Farina and Wilkins, 1980), in agreement with these findings.

Crystal Packing

The crystal packing in the monoclinic space group $P2_1$ is such that the saccharide-binding sites of the four subunits, A, B, C, and D, belonging to different molecules meet with a favorable packing of agycon groups (Fig. 2). If the tetramer is considered as a tetrahedron with the sugar-binding site of a subunit at the apex, then the packing may be described as follows: In the *ac* plane three translationally related tetrahedra touch with the A, C, and D apices, respectively. The unit cell β angle is therefore approximately 120°. The next layer of molecules along the *b* axis is related to the first layer by a 2_1 screw axis. The layers meet where the apex of the B subunit from one layer meets the other three apices of the second layer (Fig. 4).

TABLE III
Conformation of α-MUG

Subunit	φ (O5–C1–O1–C7)°	ψ (C1–O1–C7–C8)°	χ (O5–C5–C6–O6)°
A	64	0	−53
B	77	−29	−61
C	90	−115	−40
D	69	83	−52

Figure 2 shows that the molecules of α-MUG are packed so that the π-ring systems of the aglycon parts of the molecules of three subunits B, C, and D are stacked on top of each other, whereas the fourth (of subunit A) also participates in the packing, but is inclined to the rest by an angle of approximately 90°. The side chains of Tyr12 and Tyr100 and His205 are stacked against the planar aglycon group of α-MUG molecules, or each other, or against its sugar rings, in a fashion common in protein–saccharide complexes (Vyas, 1991). The stabilization of the packing arrangement is further enhanced by a number of hydrogen bonds involving water molecules located in this region, the side chains of the protein (in particular the hydroxyls of Tyr12 and Tyr100), and both oxygen atoms of the 4′-methylumbelliferyl (aglycon group) of the saccharides. The principle torsion angles for α-MUG in the four subunits are given in Table III. Although the torsion angle about the O1–C7 bond is close to 0 in subunits A and B, this eclipsed conformation is most likely stabilized by the packing and by the formation of a hydrogen bond between O22 of the aglycon and the hydroxyl of Tyr100.

Table IV shows rms deviations after a C^α superposition of the Con A tetramer in its native I222

FIG. 2. A stereo pair, drawn with the program O, showing the F_o-F_c electron density (cyan) in the region where the sugar-binding sites meet in the crystal lattice. Contouring is at 3.0 times the rms value of the electron density. The main chains of subunits A, B, C, and D are represented as rattlers and are colored blue, brown, green, and magenta, respectively. The α-MUG molecules are shown in stick representation and are colored as above. The water molecules are shown as pink spheres.

Fig. 3. A representation of the electrostatic surface potential as calculated for the A subunit by the program DELPHI and displayed using GRASP (Nicholls *et al.*, 1991; Nicholls, 1993). Negative electrostatic potential is shown in red, positive electrostatic potential in blue. (a) The bound saccharide is included in the calculation of the electrostatic surface potential. (b) The bound saccharide is shown as a stick model.

Fig. 4. Stereo pair showing the packing of four tetramers. The green tetramers are translationally related and form a layer with pseudo threefold symmetry. The blue molecule is related to one of the green ones by the crystallographic 2_1 screw operator. The labels are formed from the subunit identifier (A to D) and residue number from different tetramers that are in proximity to each other in the crystal (see text).

TABLE IV

Root Mean Square Differences (Å) in Cα Coordinates after Superposition of Pairs of Con A Structures

	α-MUG	α-PNG	α-PNM	α-MM	TriclA	TriclB
α-MUG[a]						
α-PNG	0.52					
α-PNM	0.50	0.34				
α-MM	0.49	0.64	0.65			
TriclA	0.51	0.65	0.66	0.52		
TriclB	0.57	0.52	0.52	0.58	0.46	
I222	1.03	1.25	1.25	0.88	1.13	1.29

[a] See text for code.

(Weisgerber and Helliwell, 1993) and triclinic (two tetramers per asymmetric unit, denoted TriclA, TriclB; Kanellopoulos *et al.*, 1996b) crystal forms and the complexes of Con A with α-MM (Naismith *et al.*, 1994), α-PNM, α-PNG (Kanellopoulos *et al.*, 1996a), and α-MUG (this study). Clearly, the protein tetramer is very similar in the structure of all its complexes with saccharides and in the triclinic crystal form. The tetramer in the native I222 crystal form is the obvious outlier. The change of the structure of the tetramer, going from the I222 native form to the saccharide-bound protein is, qualitatively, a movement about the center of mass of the tetramer of the A and B subunits toward each other and of the C and D subunits in the same fashion.

Structural differences between subunits occur primarily in the loops. These regions are either involved in crystal contacts (Tyr12–Pro23, Thr147–Asn153, Ile181–Ser190, Pro222–Gly231) or have little contact with other parts of the protein (Leu115–Asn124, Phe199–Ala207). The former differences are probably real and the atoms involved have relatively low temperature factors. The latter regions exhibit high

TABLE V

Metal–Ligand Distances and Saccharide Hydrogen Bonding Distances for the Four Subunits

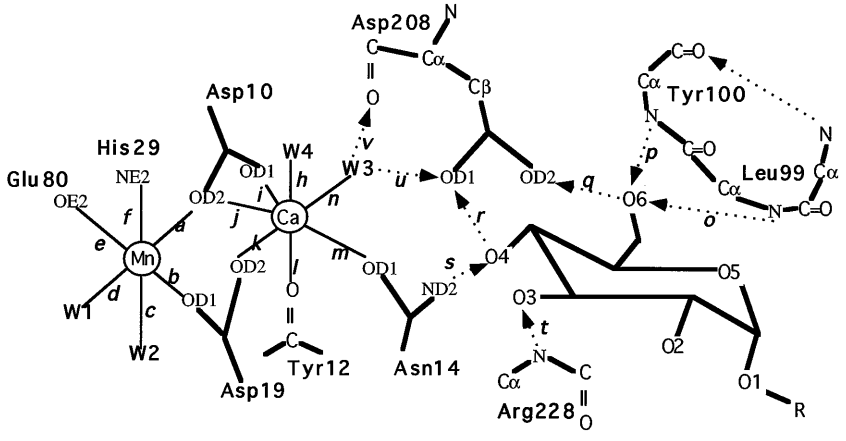

Subunit	A	B	C	D	Mean
a	2.10	2.16	2.16	2.26	2.17 (7)
b	2.13	2.16	2.16	2.20	2.16 (3)
c	2.28	2.19	2.31	2.49	2.31 (13)
d	2.14	1.93	2.11	2.21	2.10 (12)
e	2.17	2.15	2.18	2.15	2.16 (2)
f	2.27	2.33	2.24	2.18	2.25 (6)
h	2.15	2.22	2.37	2.33	2.27 (9)
i	2.26	2.38	2.38	2.42	2.36 (7)
j	2.48	2.51	2.47	2.62	2.52 (7)
k	2.38	2.31	2.20	2.34	2.31 (8)
l	2.26	2.33	2.25	2.21	2.26 (5)
m	2.42	2.36	2.35	2.26	2.35 (7)
n	2.33	2.31	2.46	2.13	2.31 (12)
o	2.93	3.14	2.85	2.92	2.96 (13)
p	3.12	3.17	2.97	3.13	3.10 (9)
q	2.97	2.92	3.21	2.89	3.00 (15)
r	2.58	2.61	2.64	2.51	2.59 (6)
s	2.82	2.88	2.71	2.90	2.83 (9)
t	2.98	3.14	3.08	2.92	3.03 (10)
u	2.75	2.79	2.70	2.82	2.77 (5)
v	3.02	3.13	2.91	3.10	3.04 (10)
O22-Y100OH	2.68	2.68			

temperature factors and the differences may simply reflect disorder and an inability to model these regions adequately.

The Glucoside-Binding Site

The higher resolution (2.78 vs 3.0 Å) and superior data quality in this structure determination relative to that of α-PNG allows the binding of a glucoside in the carbohydrate-binding site to be determined more accurately. This is schematically shown in Table V. Not surprisingly, the coordination geometry of the metals agrees with that reported for mannoside binding (Naismith *et al.*, 1994). Possible differences are shorter Mn–His24NE2 and Ca–Asp10OD2 bonds in the case of glucosides. The hydrogen bonding to the sugar is also similar except that O2 and O5 of the glucose ring have no evident hydrogen bonding partners from the protein. O2 is not involved in tight solvent-mediated contact with the protein either. The absence of hydrogen bonding between O2 and the protein, by both direct and solvent-mediated means, is the likely reason for the slightly lower affinity of Con A for glucosides relative to mannosides, where O2 can make a weak interaction with the main chain nitrogen of Leu99. There are water molecules at 3.4 and 3.2 Å from O2 in the C and D subunits, but O2 in the subunits A and B have no waters closer than 3.5 Å. It must be stressed, however, that O2 is probably solvated in solution and that the resolution of the structure determination does not allow us to make an unambiguous interpretation of the water structure. For subunits A and B (where the C1–O1–C7–C8 torsion angle is closest to 0) a hydrogen bond appears to be formed between the hydroxyl of Tyr100 and O22 of α-MUG, whereas for subunits C and D there is no such bond.

S.J.H. thanks the Supercomputing Resource for Molecular Biology (SRMB) funded by the European Union "Access to Large Scale Installations" Programme, the Greek Ministry of Research and Technology, and the University of Athens for support.

REFERENCES

Agianian, B., Perrakis, A., Kanellopoulos, P. N., Sheldrick, B., and Hamodrakas, S. J. (1996) The crystal and molecular structure of 4′-nitrophenyl-α-D-mannopyranoside ethanol solvate, submitted for publication.

Agrawal, B. B. L., and Goldstein, I. J. (1968) Protein-carbohydrate interaction. VII. Physical and chemical studies on concanavalin A, the hemagglutinin of the jack bean, *Arch. Biochem. Biophys.* **124,** 218–229.

Bourne, Y., Rouge, P., and Cambillau, C. (1992). X-ray structure of a biantennary octasaccharide-lectin complex refined at 2.3Å resolution, *J. Biol. Chem.* **267,** 197–203.

Bourne, Y., Mazurier, J. B., Legrand, D., Rouge, P., Montreuil, J., Spik, G., and Cambillau, C. (1994) Structures of a legume lectin complexed with the human lactotransferrin N2 fragment, and with an isolated biantennary glycopeptide: role of the fucose moiety, *Structure* **2,** 209–219.

Brunger, A. T. (1992a) X-PLOR Version 3.1: A System for X-ray Crystallography and NMR, Yale Univ., New Haven, CT.

Brunger, A. T. (1992b) Free R value: A novel statistical quantity for assessing the accuracy of crystal structures, *Nature* **335,** 472–475.

Delbaere, L. T. J., Vandonselaar, M., Prasad, L., Quail, J. W., Wilson, K. S., and Dauter, Z. (1993) Structures of the lectin IV of *Griffonia simplicifolia* and its complex with the Lewis b human blood group determinant at 2.0Å resolution, *J. Mol. Biol.* **230,** 950–965.

Emmerich, C., Helliwell, J. R., Redshaw, M., Naismith, J. H., Harrop, S. J., Raftery, J., Kalb(Gilboa), A. J., Yariv, J., Dauter, Z., and Wilson, K. S. (1994) High-resolution structures of single-metal-substituted concanavalin A: The Co, Ca-protein at 1.6 Å and the Ni, Ca-protein at 2.0 Å, *Acta Crystallogr.* **D50,** 749–756.

Farina, R. D., and Wilkins, R. G. (1980) Kinetics of interaction of some α- and β-D-monosaccharides with Concanavalin A, *Biochim. Biophys. Acta* **631,** 428–438.

Goldstein, I. J., and Poretz, R. P. (1986) *In* Liener, I. E., Sharon, N., and Goldstein, I. J. (Eds.), The Lectins: Properties, Functions and Applications in Biology and Medicine pp. 33–247, Academic Press, New York.

Hardman, K. D., Agarwal, R. C., and Freiser, M. J. (1982) Manganese and calcium binding sites of concanavalin A, *J. Mol. Biol.* **157,** 69–86.

Jones, T. A., Zou, J. Y., Cowan, S. W., and Kjeldgaard, M. (1991) Improved methods for building protein models in electron density maps and the location of errors in these models, *Acta Crystallogr.* **A47,** 110–119.

Kabsch, W. (1988) Evaluation of single-crystal X-ray diffraction data from a position-sensitive detector, *J. Appl. Crystallogr.* **21,** 916–924.

Kanellopoulos, P. N., Pavlou, K., Perakis, A., Agianian, B., Vorgias, C. E., Mavrommatis, C., Soufi, M., Tucker, P. A., and Hamodrakas, S. J. (1996a) The crystal structure of the complexes of concanavalin A with 4′-nitrophenyl-α-D-mannopyranoside and 4′-nitrophenyl-α-D-glucopyranoside, *J. Struct. Biol.* **116,** 345–355.

Kanellopoulos, P. N., Tucker, P. A., Pavlou, K., Agianian, B., and Hamodrakas, S. J., (1996b) A triclinic crystal form of the lectin concanavalin A, *J. Struct. Biol.* **117,** 16–23.

Kleywegt, G. J. (1996) Use of non-crystallographic symmetry in protein structure refinement, *Acta Crystallogr.* **D52,** 842–857.

Kraulis, P. J. (1991) MOLSCRIPT: A program to produce both detailed and schematic plots of protein structures, *J. Appl. Crystallogr.* **24,** 946–950.

Laskowski, R. A., MacArthur, M. W., Moss, D., and Thornton, J. M. (1993) PROCHECK: A program to check the stereochemical quality of protein structures, *J. Appl. Crystallogr.* **26,** 283–291.

Loris, R., Van Overberge, D., Dao-Thi, M. H., Poortmans, F., Maene, N., and Wyns, L. (1994) Structural analysis of two crystal forms of lentil lectin at 1.8 Å resolution, *Proteins* **20,** 330–346.

Luzatti, V. (1952) Traitement statistique des erreurs dans la determination des structures cristallines, *Acta Crystallogr.* **5,** 802–810.

Naismith, J. H., Habash, J., Harrop, S. J., Helliwell, J. R., Hunter, W. N., Wan, T. C. M., Weisgerber, S., Kalb(Gilboa), A. J., and Yariv, J. (1993) Refined structure of cadmium-substituted concanavalin A at 2.0 Å resolution, *Acta Crystallogr.* **D49,** 561–571.

Naismith, J. H., Emmerich, C., Habash, J., Harrop, S. J., Helliwell, J. R., Hunter, W. N., Raftery, J., Kalb(Gilboa), A. J., and Yariv, J. (1994) Refined structure of concanavalin A complexed with methyl-α-D-mannopyranoside at 2.0 Å resolution and comparison with the saccharide-free structure, *Acta Crystallogr.* **D50,** 847–858.

Naismith, J. H., and Field, R. A. (1996) Structural basis of

trimannoside recognition by concanavalin A, *J. Biol. Chem.* **271,** 972–976.

Navaza, J. (1994) AMoRe: An automated package for molecular replacement, *Acta Crystallogr.* **A50,** 157–163.

Nicholls, A. (1993) GRASP: Graphical Represantation and Analysis of Surface Properties, Columbia Univ., New York.

Nicholls, A., Sharp, K. A., and Honig, B. (1991) Protein folding and association: Insights from the interfacial and thermodynamic properties of hydrocarbons, *Proteins: Struct. Funct. Genet.* **11,** 281–296.

Reeke, G. N., Jr., and Becker, J. W. (1988) Carbohydrate-binding sites of plant lectins, *Curr. Topics Microbiol. Immunol.* **139,** 35–58.

Rini, J. M., Hardman, K. D., Einspahr, H., Suddath, F. L., and Carver, J. (1993) X-ray crystal structure of a pea lectin-trimannoside complex at 2.6 Å resolution, *J. Biol. Chem.* **268,** 10126–10132.

Shaanan, B., Lis, H., and Sharon, N. (1991) Structure of a legume lectin with an ordered N-linked carbohydrate in complex with lactose, *Science* **254,** 862–866.

Troganis, A. (1992) Ph.D thesis, Univ. of Athens, Greece.

Vyas, N. K. (1991) Atomic features of protein-carbohydrate interactions, *Curr. Opin. Struct. Biol.* **1,** 732–740.

Vriend, G. (1990) A molecular modelling and drug design package, *J. Mol. Graph.* **8,** 52–56.

Weisgerber, S., and Helliwell, J. R. (1993) High-resolution crystallographic studies of native concanavalin A using rapid Laue data collection methods and the introduction of a monochromatic large-angle oscillation technique (LOT), *J. Chem. Soc. Faraday Trans.* **89,** 2667–2675.